



Contents lists available at ScienceDirect

## Spectrochimica Acta Part A: Molecular and Biomolecular Spectroscopy

journal homepage: [www.elsevier.com/locate/saa](http://www.elsevier.com/locate/saa)

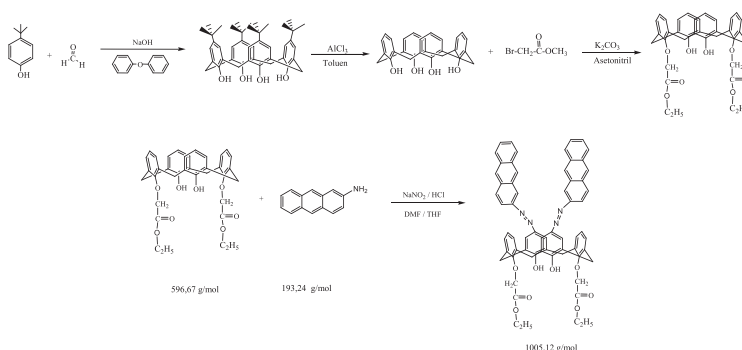
## Synthesis and DFT calculation of a novel 5,17-di(2-antracenyloxy)-25,27-di(ethoxycarbonylmethoxy)-26,28-dihydroxycalix[4]arene

A. Bayrakdar<sup>a</sup>, H.H. Kart<sup>a</sup>, S. Elcin<sup>b</sup>, H. Deligoz<sup>b</sup>, M. Karabacak<sup>c,\*</sup><sup>a</sup> Pamukkale University, Faculty of Science–Arts, Department of Physics, 20070 Denizli, Turkey<sup>b</sup> Pamukkale University, Faculty of Engineering, Department of Chemical Engineering, 20017 Denizli, Turkey<sup>c</sup> Department of Mechatronics Engineering, H.F.T. Technology Faculty, Celal Bayar University, Turgutlu, Manisa, Turkey

## HIGHLIGHTS

- 5,17-Di(2-antracenyloxy)-25,27-di(ethoxycarbonylmethoxy)-26,28-dihydroxycalix[4]arene molecule is synthesized.
- The title molecule is characterized by FT-IR, <sup>1</sup>H NMR and <sup>13</sup>C NMR spectra.
- The vibrational frequencies, chemical shifts and electronic absorption wavelengths are calculated by DFT.
- Density of the state diagrams and HOMO, LUMO energy gap for the title molecule are analyzed.

## GRAPHICAL ABSTRACT



## ARTICLE INFO

## Article history:

Received 13 July 2014

Received in revised form 17 September 2014

Accepted 19 September 2014

Available online 13 October 2014

## Keywords:

Calix[4]arene  
Molecular structure  
FT-IR  
NMR  
DFT

## ABSTRACT

In this study, 5,17-di(2-antracenyloxy)-25,27-di(ethoxycarbonylmethoxy)-26,28-dihydroxycalix[4]arene has been synthesized from 2-aminoanthracene and 25,27-dihydroxy-26,28-diethylacetate calix[4]arene. In order to identify the molecular structure and vibrational features of the prepared azocalix[4]arene, FT-IR and <sup>1</sup>H NMR spectral data have been used. FT-IR spectrum of the studied molecule is recorded in the region 4000–400 cm<sup>-1</sup>. <sup>1</sup>H NMR spectrum is recorded for 0.1–0.2 M solutions in DMSO-*d*<sub>6</sub> solution. The molecular geometry, infrared spectrum are calculated by the density functional method employing B3LYP level with different basis sets, including 6-31G(d) and LanL2DZ. The chemical shifts calculation for <sup>1</sup>H NMR of the title molecule is calculated by using by Gauge-Invariant Atomic Orbital method by utilizing the same basis sets. The total density of state, the partial density of state and the overlap population density of state diagram analysis are done via GaussSum 3.0 program. Frontier molecular orbital (HOMO–LUMO) and molecular electrostatic potential surface on the title molecule are carried out for various intramolecular interactions that are responsible for the stabilization of the molecule. The experimental results and theoretical calculations have been compared, and they are found to be in good agreement.

© 2014 Elsevier B.V. All rights reserved.

## Introduction

Calix[*n*]arenes are macrocycles prepared by the base-catalyzed condensation of *p*-*tert*-butyl phenol with formaldehyde [1]. The

cup-shaped macrocycles possess a hydrophobic cavity capable of binding organic molecules. Calixarenes belong to the important category of building blocks for supramolecular assemblies [2] and molecular recognition, and are widely used as receptors for cations [3,4], anions [5] and also neutral compounds [6]. However, there are fewer examples of complexation in solution [3] and/or in interfaces [4]. The binding properties of calix[*n*]arenes and their

\* Corresponding author. Tel.: +90 236 314 10 10; fax: +90 236 314 20 20.

E-mail address: [mehmet.karabacak@cbu.edu.tr](mailto:mehmet.karabacak@cbu.edu.tr) (M. Karabacak).

solubility in organic or aqueous solutions can be tailored by modification of the *upper rim* (*p*-position) and *lower rim* (hydroxyl).

The identification of the structure of the calix[*n*]arenes has provided further facilities to their applications in different areas. The theoretical studies of the calix[*n*]arenes have given important information about the physical and chemical properties of them. Functionalized calix[*n*]arenes have received wide attention for a variety of applications such as recovery of uranium, accelerators for instant adhesives, ionophoric electronic devices, and phase transfer agents [5–7]. Chemical modification of the *upper* or *lower rim* with alkyl groups affords amphiphilic calix[*n*]arenes [8].

Atalay and et al. [9] have carried out to calculate optimal molecular geometry, vibrational wavenumbers and modes of the free ethene-1,1,2,2-tetrayltetramethylene tetrathiocyanate. Optimized geometrical parameters and vibrational frequencies of this compound by means of HF and B3LYP with the 6-31G(d) basis set have been calculated [9]. Structure and conformational equilibrium of amino and mercaptocalix[4]arenes are studied by Suwattanamala et al. [10]. Previously, density functional theory (DFT) calculations of the electronic structure and bonding in *meso*-tetraphenylmetalporphyrins have been carried out [11]. Johansson and et al. [12,13] studied the spin distribution in low-spin iron porphyrins and compared DFT results with coupled cluster calculations for molecular spin-polarization and charge delocalization in iron porphyrins.

In recent reports [14–17], we have described the synthesis of new azocalix[*n*]arenes. By selective *p*-substitution on the *upper rim* of calix[*n*]arene, azocalix[*n*]arene (*n* = 4,6) derivatives are isolated and characterized in order to study their enol-keto tautomerization in solution and their absorption properties. In order to extend the calixarene complexing reaction to Fe<sup>3+</sup>, we have concentrated on complexation between calix[*n*]arenes (*n* = 4,6,8) and Fe<sup>3+</sup> in order to understand the important properties of calix[*n*]arene-Fe<sup>3+</sup> complexes [18].

In the present study, we have reported the synthesis, characterization and molecular structure of the title molecule. We have attempted to understand the 25,27-dihydroxy-26,28-diethylacetate-5,11-di(2-antracenyloxy)calix[4]arene. Theoretically calculated NMR parameters are shown to be very helpful in distinguishing between two (or more) related forms of the same compound, e.g. isomers and tautomers. The aim of this study is that the results obtained on the reaction of azocalix[4]arene with 2-aminoanthracene and 25,27-dihydroxy-26,28-diethylacetatecalix[4]arene are analyzed. Therefore, the molecular geometry, vibrational wavenumbers and chemical shifts in the ground state have been calculated via the DFT method.

The rest of the paper is organized as follows; experimental details and some results are presented in the Section of Experimental method. The computational detail is given in the Section of Computational method. The experimental and simulation results for structural, electronic features, chemical shifts and vibrational properties for the title molecule considered in this study are presented and discussed in the Section of Results and discussion. We have also compared the simulation results with the observed data in the same Section. Finally, the summary of our main results are given in the last section.

## Experimental method

### Generals

All solvents and compounds are commercially graded reagents and they have been used without further purification. Melting points are measured using an Electrothermal IA9100 digital melting point apparatus in capillaries sealed asunder nitrogen and are uncorrected.

### Spectra

<sup>1</sup>H NMR spectrum is recorded for 0.1–0.2 M solutions in DMSO-*d*<sub>6</sub> solution at 303 K with a Bruker AVANCE DRX 500 FT-NMR spectrometer equipped with an inverse detection 5-mm diameter broad-band probe head and z-gradient accessory working at 500.13 MHz (<sup>1</sup>H). <sup>1</sup>H NMR chemical shifts are referenced to the trace signal of CHCl<sub>3</sub> ( $\delta$  = 7.26 ppm from internal TMS). Satisfactory analytical data (0.3% for C and H) are obtained for all calix[4]arenes (1–3). FT-IR spectrum is recorded by a Perkin-Elmer 2000 FT-IR spectrophotometer (4000–400 cm<sup>-1</sup>).

### Preparation of the ligands

*p*-*tert*-Butylcalix[4]arene, calix[4]arene and 25,27-dihydroxy-26,28-diethylacetate calix[4]arene are synthesized as described by previously reported methods [19–21].

### Synthesis of the 5,17-di(2-antracenyloxy)-25,27-di(ethoxycarbonylmethoxy)-26,28-dihydroxycalix[4]arene

A solution of 2-antracenyldiazonium chloride, which is prepared from 2-aminoanthracene (0.68 g, 3.52 mmol), sodium nitrite (0.49 g, 7.04 mmol) and conc. HCl (0.85 mL) in water (3 mL), is added slowly to a cold (0 °C) solution of 25,27-diethylacetate-26,28-dihydroxycalix[4]arene (1.0 g, 1.68 mmol) and sodium acetate trihydrate (1.10 g, 8.08 mmol) in DMF-THF (50 mL, 8:5, v/v) to give a brown suspension. After keeping the suspension at (0 °C) temperature for 12 h, it is acidified with aqueous HCl (5 mL, 0.25%). The resulting mixture is then warmed up to 60 °C to keep at that temperature for 30 min to give azocalixarene (yield, 1.21 g, 72%) as a dark brown solid, which than is filtered, washed with water and MeOH. A sample for analysis is obtained as follows: azocalixarene is dissolved in 100 mL of hot aqueous NaHCO<sub>3</sub> (4.2 g) solution; to this solution is added activated charcoal (1 g). After the charcoal is filtered, the filtrate is cooled down to at room temperature and acidified with conc. HCl (1 or 2 mL). The solution is heated up to 60 °C and kept at there before cooling down for 30 min. The resulting solid is filtered, washed with water, and dried, respectively. Re-crystallization from CHCl<sub>3</sub>/EtOH mixture gives us a dark brown product (yield, 1.06 g (63%), m.p. 211–212 °C). [Found: C: 76.39%; H: 5.17%; N: 5.66%]; C<sub>64</sub>H<sub>52</sub>N<sub>4</sub>O<sub>8</sub> requires C: 76.48%; H: 5.21%; N: 5.57%. IR (KBr)  $\nu$ : 3370 cm<sup>-1</sup> (—OH), 2930 cm<sup>-1</sup> (—C—H), 1740 cm<sup>-1</sup> (—C=O), 1465 cm<sup>-1</sup> (—N=N), 1189 cm<sup>-1</sup> (C—O). <sup>1</sup>H NMR (CDCl<sub>3</sub>, 25 °C)  $\delta$ <sub>H</sub>: 1.43 (6H, t, *J* = 7.15 Hz, —CH<sub>2</sub>—CH<sub>3</sub>), 3.64 (4H, d, *J* = 13.22 Hz, Ar—CH<sub>2</sub>—Ar), 4.42 (4H, q, *J* = 7.17 Hz, —CH<sub>2</sub>—CH<sub>3</sub>), 4.58 (4H, d, *J* = 13.18 Hz, Ar—CH<sub>2</sub>—Ar), 4.81 (4H, s, O—CH<sub>2</sub>—C=O), 6.85 (2H, t, *J* = 7.59 Hz, ArH), 7.15 (4H, d, *J* = 7.63 Hz, ArH), 7.55–8.60 (22H, m, Ar—H), 8.47 (2H, s, —OH).

### Computational methods

In recent years, as a result of major advances in theoretical work, *ab initio* and DFT methods have become significantly. In particular, the elucidation of the structure of organic molecules, DFT methods according to HF methods give highly accurate results [22–26]. Therefore, DFT methods are preferred in this work. In this study, DFT/B3LYP (Becke's three-parameter hybrid model using the Lee–Yang–Parr correlation functional) level [27,28] with using 6-31G(d) and LanL2DZ basis sets is used for the explanation of molecular structure of the title molecule. Theoretical calculations are made with the Gaussian 09W package program that based on quantum chemical calculation [29]. The title molecule corresponding to the most stable geometry structure is calculated with both B3LYP/6-31G(d) and B3LYP/LanL2DZ levels. Some of the relevant

parameters are given in Table 1 and all data are given in Table S1. The optimized structure of the molecule, obtained from three dimensional GaussView 5.0.8 program [30], is given in Fig. 1. The theoretically calculated structural parameters are used for chemical shifts, vibration frequencies and the electronic properties calculation. Theoretical chemical shifts calculation for  $^1\text{H}$  NMR of the title molecule is made using by Gauge-Invariant Atomic Orbital (GIAO) method [31,32] and B3LYP level with 6-31G(d) and LanL2DZ basis sets, respectively. Solvent effect on calculated chemical shifts parameters are studied by means of the conductor-polarizable continuum model (CPCM) [33] provided by Gaussian 09 program. Highest Occupied Molecular Orbital (HOMO) and Lowest Unoccupied Molecular Orbital (LUMO) of the title molecule are calculated by the level of DFT/B3LYP with 6-31G(d) and LanL2DZ basis sets. The reactivity of the molecule determines global descriptors such as the chemical hardness, chemical softness, electron affinity, ionization potential. GaussSum 3.0 program has used to calculated contributions the molecular orbitals of functional groups in the molecule [34]. Molecular electrostatic potential surface (MEPs) are plotted to expose the chemical reactivity of molecules. The thermodynamic parameters of the title molecule such as total thermal energy, entropy, the rotational constants and heat capacity values are presented in Table S2.

## Results and discussion

### Structural analysis

The optimized molecular structure is performed at B3LYP/6-31G(d) and LanL2DZ basis sets. The studied molecule with atom numbering is shown in Fig. 1(a) and (b). The optimized molecular structure that is corresponding to the ground state belongs to  $C_1$  point group symmetry. The calculated molecular structure is

non-planar. As a result of the theoretical study, molecular structure has been determined that two hydrogen bonds are formed between the  $\text{O}(35)\text{---}\text{H}(36)\cdots\text{O}(40)$  atoms and  $\text{O}(38)\text{---}\text{H}(39)\cdots\text{H}(37)$  atoms. Hydrogen bond lengths between atoms has been calculated at 1.89195 Å and 1.82324 Å for  $\text{O}(35)\text{---}\text{H}(36)\cdots\text{O}(40)$  and  $\text{O}(38)\text{---}\text{H}(39)\cdots\text{H}(37)$ , respectively (see Scheme 1).

### Conformational analysis

In this part, to find the optimum position by the *cone* conformation, conformational analysis is made. The potential energy surface (PES) scan with the B3LYP level with 6-31G(d) basis set of theoretical computational method is done to define the preferential position of the *cone* conformation with regard to anthracene groups of the molecule. To find the most suitable conformation of the two groups, both anthracene groups separately that  $\text{C}15\text{---}\text{C}14\text{---}\text{N}80\text{---}\text{N}82$  and  $\text{C}20\text{---}\text{C}21\text{---}\text{N}79\text{---}\text{N}81$  are rotated  $360^\circ$  around the bond. The scan is made at every  $5^\circ$ . The results obtained from PES scan are given graphically in Fig. 2. The most stable structure is found to be approximately  $140^\circ$  and  $40^\circ$  for  $\text{C}20\text{---}\text{C}21\text{---}\text{N}79\text{---}\text{N}81$  and  $\text{C}15\text{---}\text{C}14\text{---}\text{N}80\text{---}\text{N}82$ , respectively. The optimized structure parameter values of  $\text{C}20\text{---}\text{C}21\text{---}\text{N}79\text{---}\text{N}81$  and  $\text{C}15\text{---}\text{C}14\text{---}\text{N}80\text{---}\text{N}82$  dihedral angles are  $141.9166^\circ$  and  $38.6532^\circ$  (see Table 1). When the results of structure parameters and potential energy surface scan are compared, it seems that they become in more suitable conformation in either anthracene groups and in the composition of the molecule structure.

### Frontier molecular orbitals (FMOs)

HOMO and LUMO which are referred as FMOs in the literature are very important parameters for computational quantum chemistry. The energy band gap is defined as the difference between

**Table 1**  
The some selected optimized structure parameters in the ground state for the title molecule.

Parameters via Gaussian	Bond length (Å)	DFT/B3LYP/6-31G(d)	DFT/B3LYP/LanL2DZ
R(1-2)	C1—C2	1.40	1.41
R(1-6)	C1—C6	1.40	1.41
R(1-41)	C1—C41	1.52	1.53
R(2-3)	C2—C3	1.39	1.40
R(2-7)	C2—H7	1.09	1.09
R(3-4)	C3—C4	1.39	1.41
R(3-8)	C3—H8	1.09	1.09
R(4-5)	C4—C5	1.40	1.41
R(4-9)	C4—H9	1.09	1.09
R(5-6)	C5—C6	1.41	1.42
Bond angles ( $^\circ$ )			
A(2-1-6)	C2—C1—C6	117.1	116.7
A(2-1-41)	C2—C1—C41	119.6	119.7
A(6-1-39)	C6—C1—C41	123.2	123.5
A(1-2-3)	C1—C2—C3	121.6	121.52
A(1-2-7)	C1—C2—H7	118.8	118.8
A(3-2-7)	C3—C2—H7	119.5	119.7
A(2-3-4)	C2—C3—C4	119.8	120.1
A(2-3-77)	C2—C3—H77	120.0	119.9
A(4-3-77)	C4—C3—H77	120.1	119.9
A(3-4-5)	C3—C4—C5	120.6	120.3
Dihedral angles ( $^\circ$ )			
D(38-18-19-47)	O38—C18—C19—C47	6.5	6.4
D(19-20-21-79)	C19—C20—C21—N79	176.8	175.2
D(47-30-31-40)	C47—C30—C31—O40	−4.4	−3.3
D(15-14-80-82)	C15—C14—N80—N82	38.6	31.1
D(20-21-79-81)	C20—C21—N79—N81	141.9	152.4
D(18-19-47-48)	C18—C19—C47—H48	−41.7	−38.2
D(18-19-20-24)	C18—C19—C20—H24	176.6	175.9
D(22-23-44-46)	C22—C23—C44—H46	−130.9	−129.8
D(27-26-50-51)	C27—C26—C50—H51	159.1	153.9
D(27-28-29-34)	C27—C28—C29—H34	−177.3	−176.8

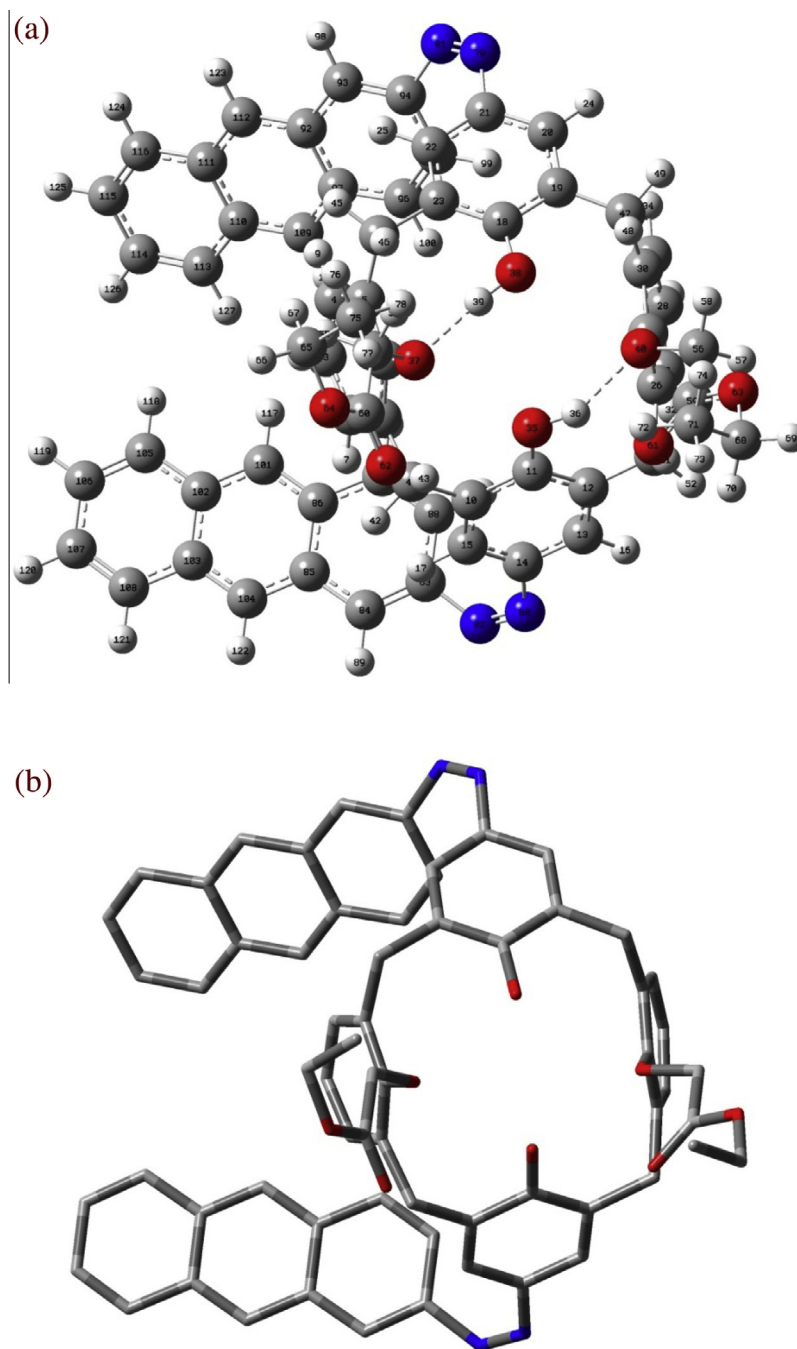
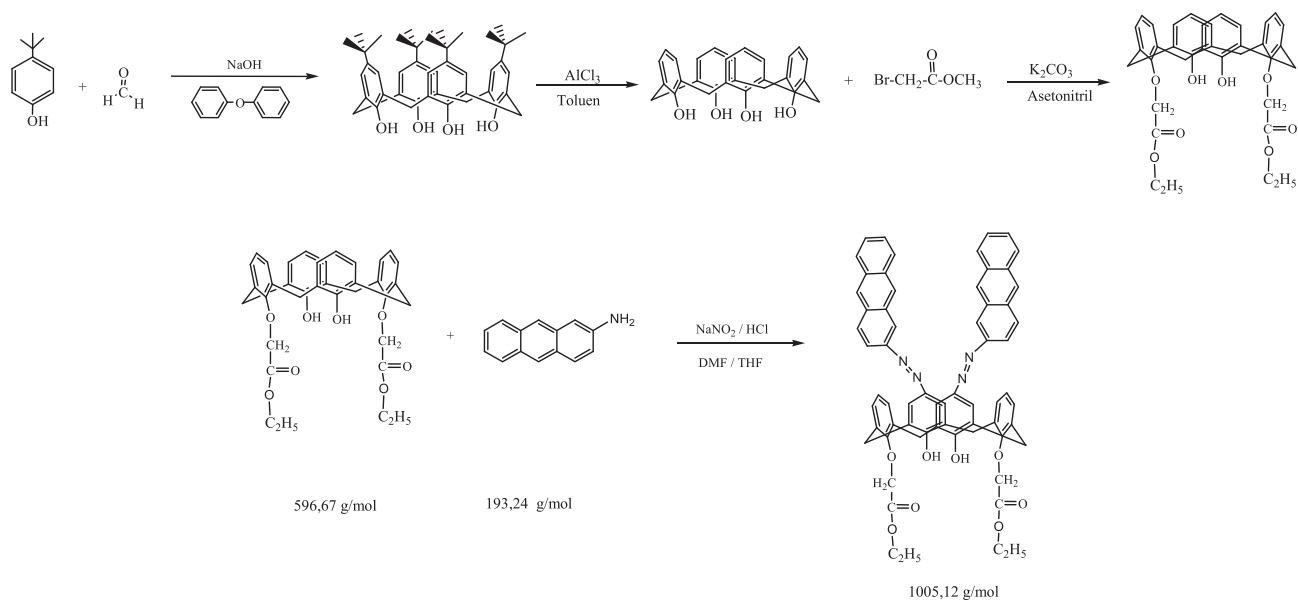


**Fig. 1.** Optimized structure with using B3LYP/6-31G(d) of the title molecule (a) Ball-bond type structure with the atomic labeling image (b) tube structure image.

HOMO and LUMO orbitals. Also the HOMO–LUMO band gap determines characteristic of the molecule such as stability of the molecule, chemical reactions, electrical and optical properties [35]. For example, the smaller the band gaps for structure the better electric conduction. Also it refers to the low kinetic stability. The ability of electron giving and accepting characterizes for HOMO and LUMO, respectively [36]. The calculations have shown that the molecule has total of 1244 molecular orbitals, 264 of these orbitals are occupied orbitals, and the rest are virtual orbitals. From these molecular orbitals, HOMO orbital is numbered 264 and LUMO orbital is numbered 265. HOMO and LUMO energies of the title molecule are calculated at  $-4.96$  eV and  $-2.08$  eV, respectively. Also that second lowest unoccupied molecular orbital (LUMO+1) and second highest unoccupied molecular orbital (HOMO–1) energy values

are calculated at  $-1.86$  and  $-5.19$  eV, respectively. Global descriptors of molecule such as chemical softness ( $S$ ), chemical hardness ( $\eta$ ), ionization potential ( $I$ ), electron affinity ( $A$ ), global electrophilicity ( $\omega$ ) and global electronegativity ( $\chi$ ) properties depend on the HOMO–LUMO orbital energies. These calculated values for molecular orbitals and global descriptors are given in Table 2. The HOMO and LUMO calculated orbitals are observed in Fig. 3.

DOS spectrum represents the number of energy level on the energy axis that the section has width  $dE$ . DOS spectrum is convoluted with Gaussian curves of heights equal to the calculated contributions for each orbital [37]. Then the spectrum is obtained here, this spectrum is referred to as partial density of state (PDOS) that shows the contribution to each molecular orbital for selected specific atoms or functional groups. Another important feature of the



**Scheme 1.** Synthesis of 5,17-di(2-antracenyloxy)-25,27-di(ethoxycarbonylmethoxy)-26,28-dihydroxycalix[4]arene.

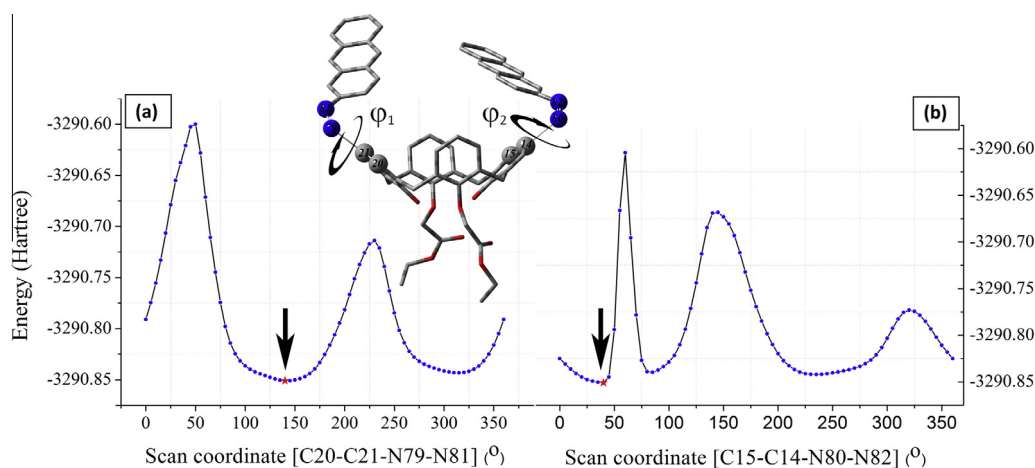


**Fig. 2.** Potential energy surface of the title molecule determined by B3LYP/6-31G(d) method. (a) For the torsion angle C20–C21–N79–N81 and (b) for the torsion angle C15–C14–N80–N82.

DOS spectrum is to show MO configuration and their contributions to chemical bonding through the overlap population density of state (OPDOS) spectrum [38]. OPDOS is also known as COOP in the literature. The COOP diagram shows the bonding, anti-bonding and nonbonding nature of the interaction of the two orbitals, atoms or groups. The positive and negative values indicate a bonding interaction and an anti-bonding interaction and zero value indicates nonbonding interactions, respectively. The total density of states (TDOS), PDOS, and OPDOS (or COOP) spectra of the title molecule are plotted in Figs. 4–6, respectively, created by convoluting the molecular orbital information with Gaussian curves of unit height and Full width at half maximum of 0.3 eV by using the GaussSum 3.0 program. GaussSum program is based on Mulliken population analysis for calculation contribution of fragment to molecular orbitals [39]. As shown in Figs. 3 and 5, LUMO electrons are mostly localized on the anthracene group having C and H atoms (60%), double-bonded nitrogen group which N=N (29%) and C<sub>6</sub>H<sub>2</sub>OH groups (11%). On the other hand HOMO electrons are mostly localized on the anthracene group having C and H atoms (49%), double-bonded nitrogen group which N=N (26%) and C<sub>6</sub>H<sub>2</sub>OH groups (25%).

**Table 2**

Frontier molecular orbital energies (eV), ionization potential (*I*), electron affinity (*A*), global electronegativity ( $\chi$ ), global electrophilicity ( $\omega$ ), total hardness ( $\eta$ ), chemical potential ( $\mu$ ) and global softness (*S*) of the title molecule are calculated by using B3LYP level with employing 6-31G(d) and LanL2DZ basis sets, respectively.

	B3LYP/6-31G(d)	B3LYP/LanL2DZ
$E_{LUMO+1}$ (eV)	−1.86	−2.13
$E_{LUMO}$ (eV)	−2.08	−2.44
$E_{HOMO}$ (eV)	−4.96	−5.10
$E_{HOMO-1}$ (eV)	−5.19	−5.41
$\Delta E_{HOMO-LUMO}$ (eV)	2.88	2.66
$\Delta E_{HOMO-LUMO+1}$ (eV)	3.10	2.97
$\Delta E_{HOMO-1-LUMO}$ (eV)	4.96	5.10
$\Delta E_{HOMO-1-LUMO+1}$ (eV)	3.33	3.28
<i>I</i> (eV)	4.96	5.10
<i>A</i> (eV)	2.08	2.44
$\chi$ (eV)	3.52	3.77
$\eta$ (eV)	1.44	1.33
<i>S</i> (eV <sup>−1</sup> )	0.35	0.38
$\mu$ (e)	8.92	9.45
$\omega$ (eV <sup>−1</sup> )	−3.52	−3.77

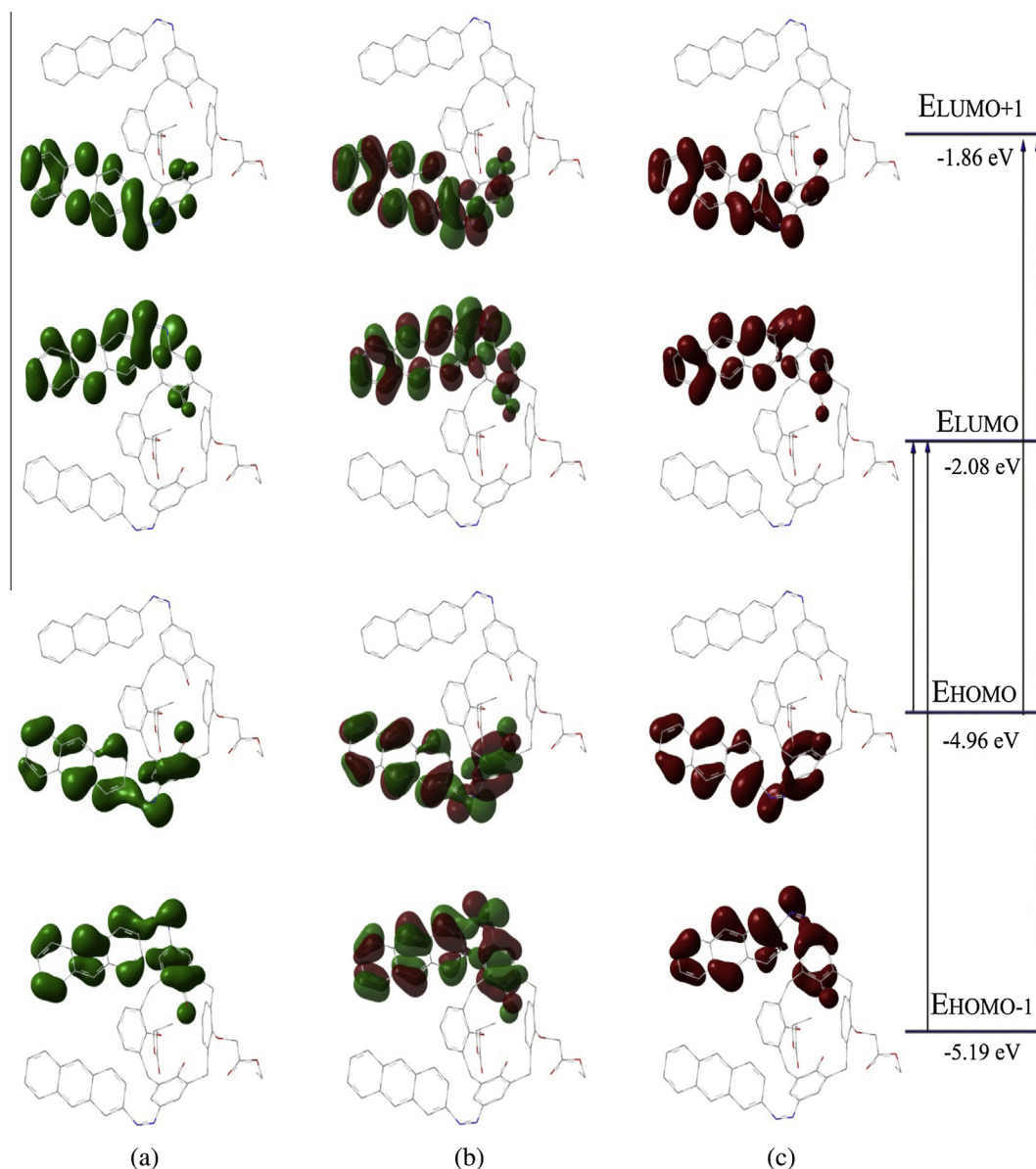


**Fig. 3.** The frontier molecular orbitals of the title molecule by using DFT/B3LYP/6-31G(d) for gas phase. (a) The only negative region of the FMOs. (b) Both positive and negative of the FMOs. (c) The only positive region of the FMOs.

The OPDOS diagrams are shown in Fig. 6 for selected groups. Accordingly, between anthracene  $\leftrightarrow$  N=N groups are shown bonding interaction, while among N=N  $\leftrightarrow$  C<sub>6</sub>H<sub>2</sub>OH groups are shown anti-bonding interaction from selected groups for LUMO energy level. However both between anthracene  $\leftrightarrow$  N=N groups and among N=N  $\leftrightarrow$  C<sub>6</sub>H<sub>2</sub>OH groups are shown anti-bonding interaction from selected groups for HOMO energy level.

#### Chemical shifts: <sup>1</sup>H and <sup>13</sup>C NMR spectra

NMR is a physical phenomenon in which nuclei in a magnetic field absorb and re-emit electromagnetic radiation. NMR spectroscopy is one of the principal techniques used to obtain physical, chemical, electronic and structural information about molecules. <sup>1</sup>H and <sup>13</sup>C NMR calculations are performed by (GIAO)/B3LYP level and 6-31G(d) and LanL2DZ basis sets for the title molecule. The solvent effect such as chloroform is included in the calculation by Gaussian 09W software program. Tetramethylsilane (TMS) is

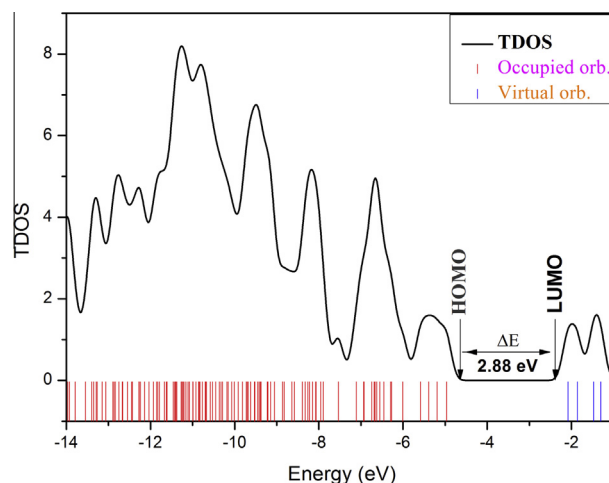


**Fig. 4.** The calculated total electronic density of the states plot for the title molecule.

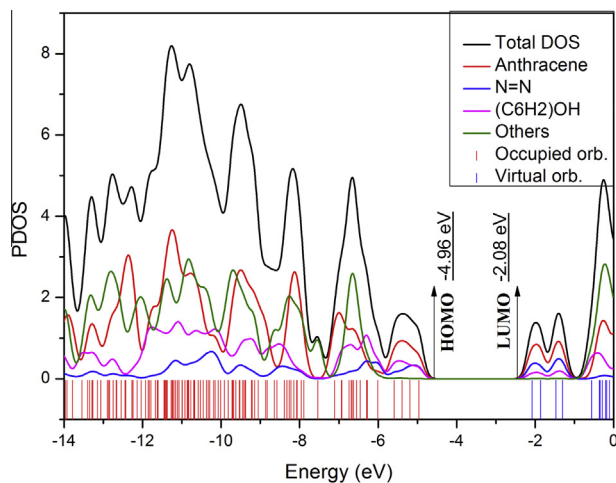


Fig. 5. The calculated partial electronic density of the states plot for the title molecule.

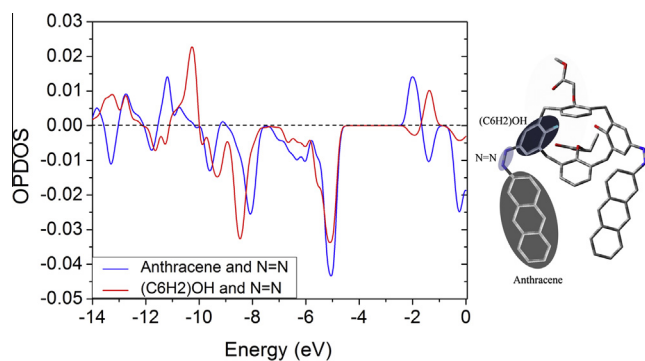


Fig. 6. The overlap population electronic density of the states plot for the title molecule.

taken into the calculation as reference for  $^1\text{H}$  and  $^{13}\text{C}$  NMR value. Chemical shift values are reported in ppm relative to TMS for  $^1\text{H}$  NMR and  $^{13}\text{C}$  NMR spectra. However, experiments on the calix[4]arenes have shown that axial (H43, H46, H48 and H51)

Table 3

Experimental and theoretical,  $^1\text{H}$  NMR isotropic chemical shifts (with respect to TMS) of the title molecule by using B3LYP level with employing 6-31G(d) and LanL2DZ basis sets.

H	Atom	B3LYP/ 6- 31G(d)	B3LYP/ LanL2DZ	Exp.	H	Atom	B3LYP/ 6- 31G(d)	B3LYP/ LanL2DZ	Exp.
7	e	5.32	6.32	7.15	69	b	3.58	3.33	4.42
8	d	6.00	6.75	6.85	70	b	4.67	4.44	4.42
9	e	5.32	5.98	7.15	72	a	1.39	1.00	1.43
16	f	7.31	7.56	7.85	73	a	0.76	0.45	1.43
17	f	5.93	6.18	7.85	74	a	1.02	0.71	1.43
24	f	7.31	7.64	7.85	76	a	0.66	0.38	1.43
25	f	5.73	5.93	7.85	77	a	1.17	0.89	1.43
32	e	6.92	6.88	7.15	78	a	0.93	0.55	1.43
33	d	6.79	6.83	6.85	89	g	7.80	7.88	8.05
34	e	6.95	7.16	7.15	90	i	7.58	7.70	8.40
36	OH	7.70	10.30	8.45	91	h	6.24	6.65	8.05
39	OH	7.17	9.64	8.45	98	g	7.91	8.00	8.05
42	AB	2.16	1.81	3.64	99	h	6.06	6.47	8.05
43	AB	5.21	5.50	4.58	100	i	7.21	7.40	8.40
45	AB	2.60	1.99	3.64	117	p	8.28	7.95	8.60
46	AB	3.13	2.61	4.58	118	n	7.80	7.69	8.05
48	AB	4.28	3.67	4.58	119	l	7.22	7.36	7.55
49	AB	3.15	2.69	3.64	120	m	7.25	7.27	7.55
51	AB	3.99	5.39	4.58	121	k	7.70	7.62	8.05
52	AB	3.19	2.78	3.64	122	o	8.12	7.94	8.60
54	c	4.63	4.46	4.81	123	o	8.21	7.98	8.60
55	c	3.67	3.29	4.81	124	n	7.85	7.66	8.05
57	c	3.76	3.98	4.81	125	l	7.49	7.33	7.55
58	c	4.59	5.00	4.81	126	m	7.62	7.46	7.55
66	b	3.65	3.49	4.42	127	k	8.22	7.82	8.05
67	b	3.58	3.40	4.42	128	p	8.31	7.99	8.60

and equatorial protons (H42, H45, H49 and H52) of bridge methylene groups in the calix[4]arene have different values of chemical shifts. This is due to the axial protons that are affected by ring current causing the resonance of the axial protons at the lower magnetic field as explained in the Ref. [40]. Experimental  $^1\text{H}$  NMR spectrum of the title molecule is given in Fig. 7. The calculated chemical shift values of  $^{13}\text{C}$  NMR are given in Table S3. The calculated and observed chemical shifts values for  $^1\text{H}$  NMR are compared in Table 3. Correlation  $R^2$  values between the calculated and the experimental values of  $^1\text{H}$  NMR for the title molecule are shown in Fig. S1 and found to be 0.9308 and 0.9209 for B3LYP/6-31G(d) and B3LYP/LanL2DZ basis sets, respectively. As can be seen

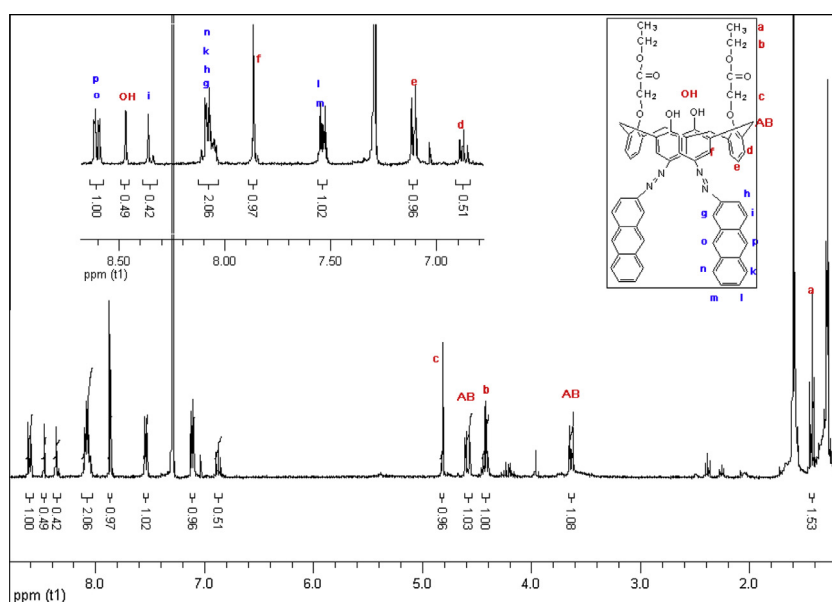


Fig. 7.  $^1\text{H}$  NMR spectrum of the title compound.

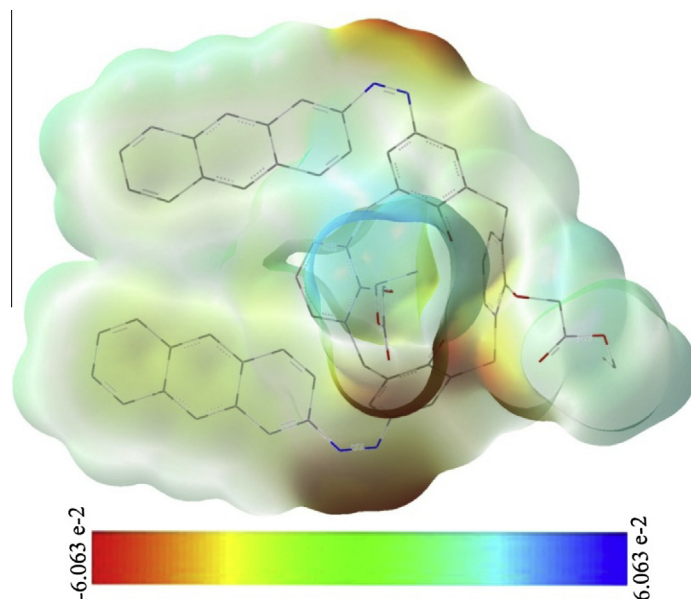


Fig. 8. The molecular electrostatic potential surface map calculated at B3LYP/6-31G(d) level.

from the values of the correlation of theoretical data are quite compatible with the experimental data.

#### Molecular electrostatic potential (MEP)

MEPs, also known as electrostatic potential maps, show that the molecules have three dimension charge distribution. In this case the knowledge of charge distribution can be used for determination of molecule interactions. Red color represents the negative region, while blue color represents the positive region and green color represents the regions of zero potential on the map (red < orange < yellow < green < blue).

MEP values are calculated by using the following equation [41];

$$V(r) = \sum_A \frac{Z_A}{|\mathbf{R}_A - \vec{r}|} - \int \frac{\rho(\vec{r}')}{|\vec{r} - \vec{r}'|} d^3r'$$

where  $Z_A$  is the charge on nucleus  $A$ , located at  $R_A$  and  $\rho(r)$  is the electronic density function of the molecule, and  $r$  is the dummy integration variable. MEPs map of the title molecule is investigated using B3LYP/6-31G(d) level of theory and are given in Fig. 8. Also that the calculated total electron density map and MEP contour plots of the title molecule are given in Fig. 9(a) and (b), respectively. While the electrophilic sites are represented as red color, the nucleophilic sites are represented as blue color. As can be seen from Fig. 8, map color range is between from  $-0.06063$  (deepest red region) to  $+0.06063$  (deepest blue region). MEPs map demonstrates that the most applicable atomic sites for electrophilic attack are N=N groups, while the most possible sites which could be involved in nucleophilic process are O–H groups.

#### Polarizability and dipole moment

The polarizabilities ( $\alpha_0$ ,  $\alpha_{xx}$ ,  $\alpha_{yy}$ ,  $\alpha_{zz}$ ,  $\alpha_{xy}$ ,  $\alpha_{xz}$  and  $\alpha_{yz}$  which are calculated by B3LYP level with 6-31G(d,p) and LanL2DZ basis sets are given in Table 4. The total dipole moment  $\mu$  is defined by;

$$\mu = (\mu_x^2 + \mu_y^2 + \mu_z^2)^{1/2}$$

The mean and anisotropy ( $\Delta\alpha$ ) of the static dipole polarizability are given as [42];

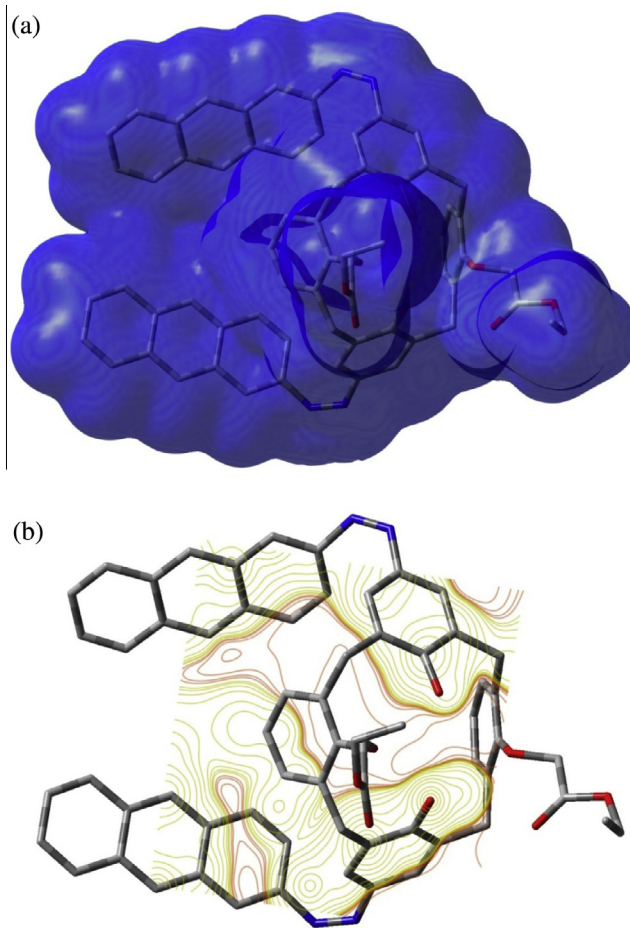


Fig. 9. (a) Total electron density surface mapped with electrostatic potential, (b) the contour map of molecular electrostatic potential surface of the title molecule predicted from DFT/B3LYP method with 6-31G(d) basis set.

$$\alpha_0 = 1/3(\alpha_{xx} + \alpha_{yy} + \alpha_{zz})$$

and

**Table 4**

The components of the polarizability ( $\alpha$ ) are reported in atomic unit (a.u.). The electric dipole moment  $\mu_0$  (in the unit of Debye), the average polarizability  $\alpha_0$  (in the unit of esu) of the title molecule is calculated from B3LYP level with using 6-31G(d) and LanL2DZ basis sets, respectively.

	DFT/B3LYP/6-31G(d)	DFT/B3LYP/LanL2DZ
$\mu_x$	3.8490	1.4771
$\mu_y$	3.6191	5.6829
$\mu_z$	5.1660	7.2559
$\mu_0$	7.3766	9.3341
$\alpha_{xx}$	1079.4780	1157.3470
$\alpha_{xy}$	55.2990	47.4860
$\alpha_{yy}$	737.9300	793.0800
$\alpha_{xz}$	-124.9490	-111.6840
$\alpha_{yz}$	22.9920	0.5940
$\alpha_{zz}$	563.6920	570.8720
$\alpha_0$	117.6263	124.5522
$\Delta\alpha$	67.3495	76.0036

$$\Delta\alpha = \frac{1}{\sqrt{2}} \left[ (\alpha_{xx} - \alpha_{yy})^2 + (\alpha_{yy} - \alpha_{zz})^2 + (\alpha_{zz} - \alpha_{xx})^2 + 6\alpha_{xz}^2 + 6\alpha_{xy}^2 + 6\alpha_{yz}^2 \right]^{\frac{1}{2}}$$

The polarizability values are expressed in the atomic unit (a.u.) obtained from Gaussian output file. Then, these calculated values are converted to electrostatic unit with 1 a.u. = 0.1482 × 10<sup>-24</sup> esu. The components of the polarizability and electric dipole moment are given in Table 4.

The calculated dipole moment values by using B3LYP/6-31G(d) and B3LYP/LanL2DZ levels of DFT method are computed as 7.3766 and 9.3341 Debye, respectively. Also the total polarizability values for the title molecule are calculated at 117.6263 × 10<sup>-24</sup> esu and 124.5522 × 10<sup>-24</sup> esu for the B3LYP with 6-31G(d,p) and LanL2DZ basis sets, respectively.

#### Vibrational frequencies analysis

The main purpose in vibration analysis is to find the vibration modes depending on the geometry of the ground state of

molecular structure. The Gaussian 09W package program is used to calculate theoretical vibration frequencies. In studies with Gaussian 09W package program, calculations are done in the gas phase while the experiment is performed for the solid sample and without taking into account anharmonic effects. Therefore the calculated values are disagreement with experimentally observed ones. The theoretically calculated results are scaled with the scaling factor to eliminate this discrepancy. The B3LYP level of DFT method yields a good agreement of harmonic vibrational frequencies for small and medium-sized molecules [43–45]. In this study, the theoretically vibrational wavenumber calculations are performed by using Gaussian 09W package at the DFT/B3LYP level with the basis sets of 6-31G(d) and LanL2DZ. The theoretically calculated vibrational frequencies are scaled by 0.961 for both 6-31G(d) and LanL2DZ basis sets [46]. The title molecule is composed of 128 atoms, but it does not have a planar structure. Therefore, the title molecule has 378 (3N-6) normal modes of vibrations. The theoretical calculation results, scaled, unscaled vibrational frequencies, IR intensities and the comparison of scaled frequencies with experimentally observed frequencies are given in Table 5 and Fig. 10. Also the assignment of the vibrations are made with the help of the GaussView 5.0.8 molecular visualization program and interpreted by means of PED by using VEDA 4 program [47]. The assignment data are also given in Table 5. The correlation values between the experimental and calculated vibrational frequencies are found to be 0.9997 and 0.9964. The correlation graphs are shown in Fig. S2 (a) and (b) for 6-31G(d) and LanL2DZ basis sets, respectively.

#### O–H Vibration

Hydroxy group exhibits stretching vibrational motion. Molecular structure has a free hydroxyl group or if does not include hydrogen bonding, stretching band strongly in the region 3550–3700 cm<sup>-1</sup> [48]. The structure has phenol groups and if it has hydrogen bond, the OH stretching band would be reduced towards to 3200–3550 cm<sup>-1</sup> region [49,50]. According to theoretical calculation, there are two hydrogen bonds in the molecular

**Table 5**

Selected vibrational wavenumbers obtained from B3LYP level with using 6-31G(d) and LanL2DZ basis sets in cm<sup>-1</sup>, experimental frequencies from FT-IR spectrum in cm<sup>-1</sup>, IR Intensities (km mol<sup>-1</sup>) and assignment with PED percentage in square brackets.

Modes	B3LYP/LanL2DZ			B3LYP/6-31G(d)			Exp.	Assignment (%)
	Unscaled	Scaled	Intensity	Unscaled	Scaled	Intensity		
84	486	468	6.61	482	463	3.87	466	Butterfly CHring(35) + $\delta$ {CC–CH <sub>3</sub> }(13) + $\delta$ CCN(10)
92	514	494	1.03	513	493	6.07	494	$\delta$ CCN(15) + $\beta$ OCOC(12)
103	573	551	12.75	573	551	9.46	554	$\delta$ CCC(12)
112	627	603	1.63	619	594	66.80	596	$\delta$ OCO(15) + $\delta$ COC(10)
120	676	650	17.57	666	640	40.79	642	$\tau$ HOCC(34) + $\nu$ COH(15)
134	782	751	52.07	767	737	12.70	737	$\tau$ HCCC(37)
142	810	779	31.73	791	760	2.66	767	$\tau$ CCCH(65) + $\delta$ CCC(11)
156	877	843	107.37	861	827	1.17	829	$\tau$ CCCH(65)
175	965	927	8.76	935	899	15.61	900	$\tau$ HCCC(31) + $\gamma$ CH <sub>2</sub> (16)
178	971	933	8.00	948	911	16.10	951	$\tau$ HCCC(36) + $\gamma$ CH <sub>2</sub> (28)
202	1059	1018	243.32	1090	1047	133.98	1055	$\nu$ Cring(20) + $\delta$ CCHring(13) + $\nu$ CO(27)
208	1122	1079	240.49	1129	1085	61.59	1086	$\delta$ OCC(48) + $\omega$ CH <sub>2</sub> (19)
213	1142	1098	13.87	1160	1115	221.51	1115	$\nu$ CO(45) + $\gamma$ CH <sub>2</sub> (22)
226	1210	1164	2.51	1209	1161	24.39	1159	$\nu$ CO(18) + $\gamma$ CH <sub>2</sub> (15)
232	1232	1185	5.80	1240	1191	286.08	1189	$\nu$ CO(54) + $\delta$ COH(15) + $\gamma$ CH <sub>2</sub> (15) + $\omega$ CH <sub>2</sub> (13)
248	1309	1259	47.43	1308	1257	73.23	1258	$\nu$ CH <sub>2</sub> (19) + $\delta$ COH(15) + $\delta$ CCH(14)
267	1398	1344	2.04	1403	1348	3.18	1344	$\nu$ CC(51) + $\delta$ HCC(30)
273	1441	1385	19.28	1433	1377	0.26	1378	$\delta$ HCC(28) + $\nu$ CC(21)
306	1540	1481	5.66	1576	1514	106.64	1465	$\nu$ NN(51) + $\nu$ CC(25) + $\delta$ HCC(18)
319	1644	1580	9.17	1652	1587	60.60	1587	$\nu$ Cring(20) + $\delta$ CCHring(15) + $\nu$ NN(11)
325	1707	1641	198.66	1829	1758	259.24	1740	$\nu$ C=O(84) + $\nu$ CH(11)
328	3053	2935	35.82	3048	2929	37.41	2930	$\nu_{\text{sym}}$ CH <sub>2</sub> (81)
338	3131	3010	14.19	3099	2978	25.97	2980	$\nu_{\text{sym}}$ CH <sub>2</sub> (91)
349	3184	3061	1.16	3170	3047	9.05	3045	$\nu$ CH(81)
377	3261	3135	868.73	3545	3406	641.06	3370	$\nu$ OH(99)

$\nu$ : stretching,  $\nu_{\text{sym}}$ : symmetric stretching,  $\delta$ : in plane bending,  $\omega$ : wagging,  $\tau$ : torsion,  $t$ : twisting,  $\gamma$ : rocking,  $s$ : scissoring,  $\beta$ : out of bending.

structure. One of them is between O38–H39...O37, the other one is between O35–H36...O40. The O–H stretching vibration is observed at  $3370\text{ cm}^{-1}$  in vibration spectrum (FT-IR), while this vibration mode is calculated at  $3406\text{ cm}^{-1}$  for B3LYP/6-31G(d) level and  $3135\text{ cm}^{-1}$  for B3LYP/LanL2DZ level with the 99% contribution of PED. The theoretical results are in good agreement with the experimental results.

#### C–H Vibration

C–H stretching vibrations in infrared spectrum of molecular structures are generally observed in the range of  $3100\text{--}3000\text{ cm}^{-1}$  [51,52]. Also CH stretching vibrations in  $\text{CH}_2$  and  $\text{CH}_3$  groups for the most part show up in the region  $3000\text{--}2850\text{ cm}^{-1}$  [53–55]. In this work, the bands of C–H stretching vibrations are observed at  $2930\text{ cm}^{-1}$ ,  $2980\text{ cm}^{-1}$  and  $3049\text{ cm}^{-1}$  in FT-IR. We have calculated C–H vibrations at  $2929\text{ cm}^{-1}$ ,  $2978\text{ cm}^{-1}$ ,  $3047\text{ cm}^{-1}$  and  $2935\text{ cm}^{-1}$ ,  $3010\text{ cm}^{-1}$ ,  $3061\text{ cm}^{-1}$  for DFT/B3LYP level with 6-31G(d) and LanL2DZ basis sets, respectively.

#### C=O Vibration

The C=O group of bands, the functional groups, are one of the most pronounced on spectrum. The C=O band is assigned strong

stretching motion ranging from  $1600\text{ cm}^{-1}$  to  $1800\text{ cm}^{-1}$  [56–58]. In this study, the group vibration band of the C=O is observed at  $1740\text{ cm}^{-1}$  experimentally, while this vibration mode is calculated at  $1758\text{ cm}^{-1}$  for B3LYP/6-31G(d) level and  $1641\text{ cm}^{-1}$  for B3LYP/LanL2DZ level with the 84% contribution of PED.

#### N=N Vibration

N=N stretching vibration mode is a kind of a very strong bond which is exhibit stretching motion. In this work, the experimental value is observed at  $1465\text{ cm}^{-1}$  for the title molecule. Whereas the calculated values are found to be  $1514\text{ cm}^{-1}$  and  $1481\text{ cm}^{-1}$  using by DFT/B3LYP level with 6-31G(d) and LanL2DZ basis sets, respectively.

#### C–O Vibration

The stretching vibrations bands of C–O groups produce a strong band in the region of  $1260\text{--}1000\text{ cm}^{-1}$  [59]. In this work, the experimental value is assigned at  $1189\text{ cm}^{-1}$  from vibrational frequencies spectrum of the title molecule. On the other hand, we have computed C–O band at  $1191\text{ cm}^{-1}$  for B3LYP/6-31G(d) and  $1185\text{ cm}^{-1}$  for B3LYP/LanL2DZ basis sets according to theoretically calculation for the title molecule. The theoretical result

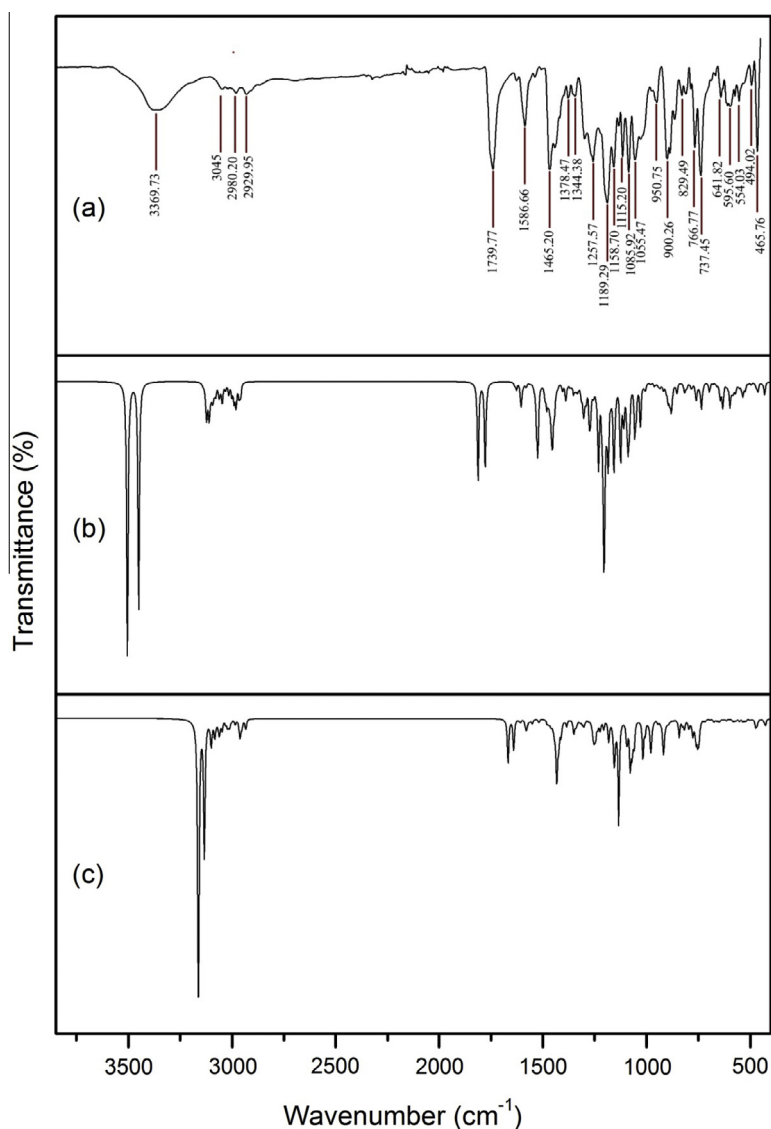


Fig. 10. (a) Experimental FT-IR spectrum, (b) calculated infrared spectrum by using B3LYP/6-31G(d) (c) calculated infrared spectrum by using B3LYP/LanL2DZ.

(1185 cm<sup>-1</sup>) is in good agreement with the experimental result (1189 cm<sup>-1</sup>).

Generally, it is difficult to assign all bands due to the complexity of the vibration bands. In this study, it is shown that only characteristic stretching vibration bands can be identified.

## Conclusions

In this paper, the title molecule is synthesized and characterized by FT-IR and <sup>1</sup>H NMR spectroscopic techniques. Additionally, DFT calculations for the title molecule are presented for the first time. Theoretical calculations are used for the characterization of the title molecule. All theoretical calculations are performed with DFT/B3LYP level, 6-31G(d) and LanL2DZ basis sets. The complete molecular structural parameters of the optimized geometry of the title molecule have been obtained from theoretical calculations by helping Gaussian 09W package program. The calculated and scaled wavenumbers are compared with the experimental wavenumbers. The complete vibrational spectra are also assigned by means of the PED analyses determined from the VEDA 4 and GaussView softwares. The good compatible has been observed between the experimental and scaled frequencies obtained by using the basis set 6-31G(d). In order to understand the charge transfer in the molecule, frontier molecular orbital are presented. On the other hand, from MEP of the title molecule, the negative region is mostly localized on the hydroxyl group, while positive region is on the N=N bond having N atoms. The contribution of groups to molecular orbitals is determined with helping TDOS and PDOS graphs that are obtain using by GaussSum program. Theoretical <sup>13</sup>C and <sup>1</sup>H magnetic isotropic chemical shifts values (with respect to TMS) are reported and compared with experimental data, showing a very good agreement <sup>1</sup>H NMR.

## Acknowledgement

This study has been supported by Pamukkale University (Grant Nos: 2012FBEO02, 2012FBEO50, 2013FBEO09, 2013FBEO13).

## Appendix A. Supplementary material

Supplementary data associated with this article can be found, in the online version, at <http://dx.doi.org/10.1016/j.saa.2014.09.074>.

## References

- [1] C.D. Gutsche, Calixarenes, Royal Society of Chemistry, Cambridge, England, 1989.
- [2] L. Wang, M.O. Vysotsky, A. Bogdan, M. Bolte, V. Böhmer, *Science* 304 (2004) 1312.
- [3] A. Ikeda, S. Shinkai, *J. Am. Chem. Soc.* 116 (1994) 3102.
- [4] J.W. Steed, J.L. Atwood, *Supramolecular Chemistry*, Wiley-VCH, Chichester, 2000.
- [5] W. Abraham, *J. Incl. Phenom. Macrocycl. Chem.* 43 (2002) 159.
- [6] C.D. Gutsche, I. Alam, *Tetrahedron* (1988) 4689.
- [7] M. Orda-Zgadaj, V. Wendel, M. Fehlinger, B. Ziemer, W. Abraham, *Eur. J. Org. Chem.* (2001) 1549.
- [8] G. Deng, T. Sakaki, Y. Kawahara, S. Shinkai, *Tetrahedron Lett.* 33 (1992) 2163.
- [9] Y. Atalay, K. Sancak, D. Avci, *J. Mol. Struct.: Theochem.* 774 (2006) 33–34.
- [10] A. Suwattanamala, A.L. Magalhães, J.A.N.F. Gomes, *Chem. Phys.* 310 (2005) 109–122.
- [11] M.S. Liao, S. Scheiner, *J. Chem. Phys.* 117 (2002) 205.
- [12] M.P. Johansson, D. Sundholm, G. Gerfen, M. Wikstrom, *J. Am. Chem. Soc.* 124 (2002) 11771.
- [13] M.P. Johansson, D. Sundholm, *J. Chem. Phys.* 120 (2004) 3229.
- [14] H. Deligoz, N. Ercan, *Tetrahedron* 58 (14) (2002) 2881–2884.
- [15] F. Karci, I. Sener, H. Deligoz, *Dyes Pigments* 59 (2003) 53–61.
- [16] I. Sener, F. Karci, E. Kılıç, H. Deligoz, *Dyes Pigments* 62 (2004) 141–148.
- [17] T. Tilki, I. Sener, F. Karci, A. Gülce, H. Deligoz, *Tetrahedron* 61 (40) (2005) 9624–9629.
- [18] H. Deligoz, *J. Incl. Phenom. Macrocycl. Chem.* 55 (2006) 197.
- [19] C.D. Gutsche, M. Iqbal, *Org. Synth.* 68 (1990) 234–238.
- [20] C.D. Gutsche, M. Iqbal, D. Stewart, *J. Org. Chem.* 51 (1986) 742–745.
- [21] E.M. Collins, M.A. McKevey, E. Madigan, M.B. Moran, *J. Chem. Soc. Perkin Trans. 1* (1991) 3137–3142.
- [22] M. Karakus, S. Solak, T. Hökelek, H. Dal, A. Bayraktar, S. Özdemir Kart, M. Karabacak, H.H. Kart, *Spectrochim. Acta A* 122 (2014) 582–590.
- [23] M.A. Palafox, G. Tardajos, A.G. Martines, V.K. Rastogi, D. Mishra, S.P. Ojha, W. Kiefer, *Chem. Phys.* 340 (2007) 17–31.
- [24] M. Karabacak, E. Sahin, M. Cinar, I. Erol, M. Kurt, *J. Mol. Struct.* 886 (2008) 148–157.
- [25] F. Ucu, V. Guclu, A. Saglam, *Spectrochim. Acta A* 70 (2008) 524–531.
- [26] M. Karabacak, A. Coruh, M. Kurt, *J. Mol. Struct.* 892 (2008) 125–131.
- [27] C. Lee, W. Yang, R.G. Parr, *Phys. Rev. B* 37 (1988) 785–789.
- [28] A.D. Becke, *J. Chem. Phys.* 98 (1993) 5648–5652.
- [29] M.J. Frisch et al., *Gaussian 09, Revision A.1*, Gaussian Inc., Wallingford CT, 2009.
- [30] R.D. Dennington, T.A. Keith, J.M. Millam, *GaussView 5*, Gaussian Inc., 2008.
- [31] R. Ditchfield, *J. Chem. Phys.* 56 (1972) 5688–5691.
- [32] K. Wolinski, J.F. Hinton, *J. Am. Chem. Soc.* 112 (1990) 8251–8260.
- [33] V. Barone, M. Cossi, *J. Phys. Chem. A* 102 (1998) 1995–2001.
- [34] N.M. O'Boyle, A.L. Tenderholt, K.M. Langner, *J. Comput. Chem.* 29 (2008) 839–845.
- [35] C.V. Filip, S. Miclaus, *J. Mol. Struct.* 744 (2005) 363.
- [36] G. Gece, *Corros. Sci.* 50 (2008) 2981–2992.
- [37] N.M. O'Boyle, Ph.D. Thesis, Dublin City University, 2004.
- [38] M. Karabacak, E. Kose, A. Atac, A.M. Asiri, M. Kurt, *J. Mol. Struct.* 1058 (2014) 79–96.
- [39] R.S. Mulliken, *J. Chem. Phys.* 23 (1955) 1833.
- [40] C.D. Gutsche, B. Dhawan, J.A. Levine, K.H. No, L. Bauer, *Tetrahedron* 39 (1983) 409–426.
- [41] P. Politzer, J.S. Murray, *Theor. Chem. Acc.* 1087 (2002) 134–142.
- [42] V. Keshari, W.M.K.P. Wijekoon, P.N. Prasad, S.P. Karna, *J. Phys. Chem.* 99 (22) (1995) 9045–9050.
- [43] S. Sudha, N. Sundaraganesan, M. Kurt, M. Cinar, M. Karabacak, *J. Mol. Struct.* 985 (2011) 148–156.
- [44] N.C. Handy, P.E. Masley, R.D. Amos, J.S. Andrews, C.W. Murray, G. Laming, *Chem. Phys. Lett.* 197 (1992) 506–515.
- [45] G. Bakalarski, B. Lesyng, *Pol. J. Chem.* 72 (1998) 1792–1797.
- [46] <http://cccbdb.nist.gov/vibscalejust.asp>.
- [47] M.H. Jamroz, *Vibrational Energy Distribution Analysis VEDA 4*, Warsaw, 2004.
- [48] A. Teimouri, A.N. Chermahini, K. Taban, H.A. Dabbagh, *Spectrochim. Acta A* 72 (2009) 369–377.
- [49] H.A. Dabbagh, A. Teimouri, A.N. Chermahini, M. Shahraki, *Spectrochim. Acta A* 69 (2008) 449–459.
- [50] D. Mahadevan, M. Karabacak, S. Periandy, S. Ramalingam, *Spectrochim. Acta A* 86 (2012) 139–151.
- [51] V. Krishnakumar, R. John Xavier, *Indian J. Pure Appl. Phys.* 41 (2003) 597.
- [52] A. Coruh, F. Yilmaz, B. Sengez, M. Kurt, M. Cinar, M. Karabacak, *Struct. Chem.* 22 (2011) 45–56.
- [53] E. Pretsch, P. Bühlmann, C. Affolter, *Structure Determination of Organic Compounds: Tables of Spectral Data*, third ed., Springer-Verlag, Berlin, Heidelberg and New York, 2000.
- [54] G. Socrates, *Infrared Characteristic Group Frequencies*, third ed., Wiley Interscience Publications, New York, 1980.
- [55] S. Ramalingam, A. Jayaprakash, S. Mohan, M. Karabacak, *Spectrochim. Acta A* 82 (2011) 79–90.
- [56] G. Varsanyi, *Vibrational Spectra of Benzene Derivatives*, Academic Press, New York, 1969.
- [57] G. Socrates, *Infrared and Raman Characteristic Group Wavenumbers-Tables and Charts*, third ed., John Wiley and sons, New York, 2001.
- [58] A. Atac, M. Karabacak, E. Kose, C. Karaca, *Spectrochim. Acta A* 83 (2011) 250–258.
- [59] M. Kubinyi, F. Billes, A. Grofcsik, G. Keresztury, *J. Mol. Struct.* 266 (1992) 339–344.